Electronic Supplementary Material (ESI) for ChemComm.

Supporting information

Bulk ferromagnetism in cleavable van der Waals telluride $NbFeTe_2$

Anna V. Stepanova,[a] Andrei V. Mironov,[a] Alexey V. Bogach,[b] Andrey N. Azarevich,[b] Igor A. Presniakov,[a,c] Alexey V. Sobolev,[a,c] Denis A. Pankratov,[a] Vladimir A. Zayakhanov,[d] Sergey S. Starchikov,[d] Valeriy Yu. Verchenko,[a,*] and Andrei V. Shevelkov[a]

[a]Department of Chemistry, Lomonosov Moscow State University, 119991 Moscow, Russia.
[b]Prokhorov General Physics Institute of the Russian Academy of Sciences, 119991 Moscow, Russia.
[c]MSU-BIT University, Shenzhen, 517182 Guangdong Province, P. R. China
[d]National Research Centre "Kurchatov Institute", 123182 Moscow, Russia.

e-mail: valeriy.verchenko@gmail.com.

Experimental details

For the synthesis of single crystals, we used chemical vapor transport reactions. Nb (powder, 99.8%, Sigma-Aldrich), Fe (powder, 99%, Merck), and Te (pieces, 99.999%, Sigma-Aldrich) in the stoichiometric molar ratio ν(Nb):ν(Fe):ν(Te) = 1:1:2 (total mass = 0.5 g) were loaded inside a quartz ampule (8 mm inner diameter, 200 mm length) along with iodine, which was used as a transport agent (20 mg of I_2 that corresponds to concentration of 5 μmol/mL). The ampule was sealed under vacuum of 5×10^{-3} mbar and placed in a horizontal two-zone programmable furnace. The direct temperature gradient of 800-700°C for two weeks was used. A polycrystalline sample was obtained using annealing of the stoichiometric mixture of elements at 900°C, followed by grinding of the specimen in an agate mortar and second annealing at 700°C with subsequent quenching in water.

Single crystals of $NbFeTe_2$ were investigated on a Bruker D8 Quest single-crystal X-ray diffractometer equipped with a PHOTON III detector, a charge-integrating pixel array detector (CPAD), a laterally graded multilayer (Goebel) mirror, and a microfocus Mo-target X-ray tube (λ = 0.73071 Å). Crystal structure was solved using Charge Flipping method and subsequently refined against $|F|$ in the full-matrix anisotropic approximation using the Jana 2006 package [1]. The multiscan routine was used for the absorption correction. Details of data collection and refinement of crystal structure are listed in Table S1. Atomic position parameters and selected interatomic distances are summarized in Tables S2 and S3, respectively.

Powder X-ray diffraction (PXRD) patterns of polycrystalline $NbFeTe_2$ were investigated on a Huber G670 Guinier camera ($CuK\alpha_1$ radiation, Ge_{111} monochromator). The STOE WinXPOW program (version 1.06) was used for data processing. Rietveld refinements of the crystal structure against X-ray powder diffraction data were performed using the Jana 2006 software [1]. The previously obtained single-crystal X-ray diffraction data were used as a starting model.

Elemental composition of single crystals was examined by electron probe microanalysis (EPMA) on a JSM JEOL 6490-LV scanning electron microscope equipped with an energy dispersive X-ray detection system INCA x-Sight. Data were collected and averaged from 10 point spectra for each sample. Elemental Co was used as a standard.

Magnetization measurements were performed on the oriented single crystals employing a Magnetic Properties Measurement System (MPMS-XL5, Quantum Design). Magnetic moment was measured under the zero-field-cooling and field-cooling conditions at temperatures between 2 K and 300 K in 0.01 T, 0.1 T, 1 T, and 5 T magnetic fields. Isothermal magnetization measurements were performed under the zero-field-cooling conditions by sweeping magnetic field between -5 T and 5 T at various temperatures. Data obtained for a single crystal with magnetic field applied in the in-plane direction and for polycrystalline sample are shown in Figure S2.

Electronic structure calculations were performed within the framework of the density functional theory using the full-potential local-orbital minimum-basis band-structure code FPLO (version 14.00-47) [2]. The experimental structural data based on single-crystal X-ray diffraction measurements were used in calculations. In the scalar relativistic regime, general gradient approximation was used to treat the exchange and correlation energy [3]. Integrations were performed by the improved tetrahedron method [4] on a grid of 12×12×12 *k*-points in the first Brillouin zone.

Mössbauer spectra were measured with an electrodynamic-type spectrometer MS-1104Em operated in the constant acceleration mode and equipped with a cryostat [5]. The ^{57}Co(Rh) γ-ray source was kept at room temperature. The values of the isomer shift are given relative to α-Fe at room temperature. Experimental spectra were processed using the "SpectrRelax" program [6]. Electric field gradient parameters were computed using the "GradientNCMS" software designed by the authors, more details are given in Ref. [7].

Crystal structures of monoclinic $NbFeTe_2$ and orthorhombic $Nb_{0.9}Fe_{0.9}Te_2$

The orthorhombic form of $NbFeTe_2$ was reported in two studies, where similar synthetic conditions were used [8,9]. In Ref. [8], the compound was synthesized by annealing the Nb, Fe, and Te mixture with the 2:3:5 molar ratio at 850 °C for 5 days using $TeCl_4$ as a transport agent. In Ref. [9], the 2:3:5.5 mixture of Nb, Fe, and Te, respectively, was annealed in a temperature gradient of 800-700 °C using iodine as a transport agent. According to the crystal structure refinement, the Nb and Fe crystallographic positions are partially occupied yielding the $Nb_{0.9}Fe_{0.9}Te_2$ composition [9]. $Nb_{0.9}Fe_{0.9}Te_2$ crystallizes in the orthorhombic unit cell, *Pmna* space group, with the unit cell parameters of a = 7.951(2) Å, b = 7.241(1) Å, and c = 6.233(1) Å [9]. Similar structural parameters are reported in Ref. [8]. The crystal structures of monoclinic $NbFeTe_2$ (this study) and orthorhombic $Nb_{0.9}Fe_{0.9}Te_2$ [8,9] are shown in Figure S1. The top view on the structural layer is presented.

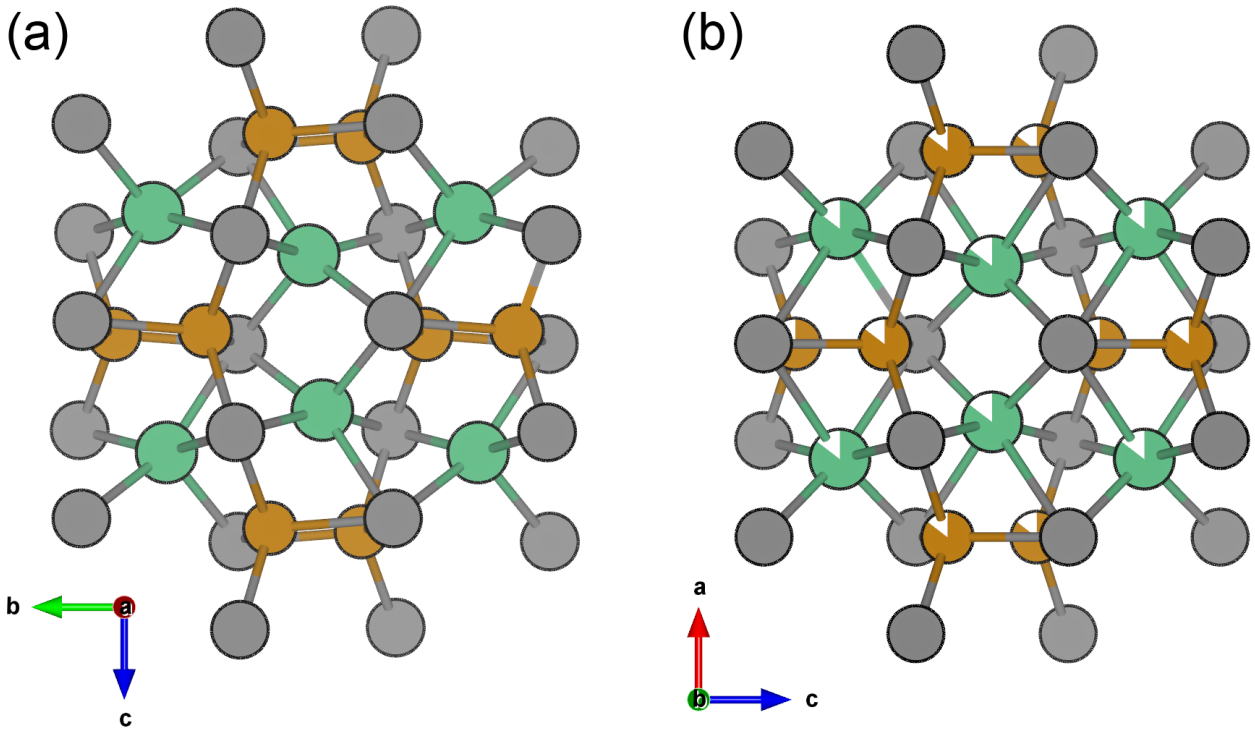

Figure S1 Crystal structures of monoclinic $NbFeTe_2$ (a) [this study] and orthorhombic $Nb_{0.9}Fe_{0.9}Te_2$ (b) [8,9]. Nb, Fe, and Te atoms are shown in green, brown, and gray, respectively.

Monoclinic $NbFeTe_2$ and orthorhombic $Nb_{0.9}Fe_{0.9}Te_2$ have slightly different composition, similar atomic environment, but significantly different interatomic distances. In particular, $Nb@Te_6$ distorted octahedra in orthorhombic $Nb_{0.9}Fe_{0.9}Te_2$ show Nb-Te contacts of 2.77-3.27 Å [8], while in monoclinic $NbFeTe_2$ one Nb-Te distance is 3.70 Å, and thus, Nb centers the $Nb@Te_5$ pyramids. Two scenarios can be proposed to explain the relationship between these phases: (i) monoclinic $NbFeTe_2$ and orthorhombic $Nb_{0.9}Fe_{0.9}Te_2$ are thermodynamically stable individual compounds, (ii) there is a $Nb_{1-x}Fe_{1-x}Te_2$ solid solution-like phase with the orthorhombic-to-monoclinic structural phase transition driven either by the change of composition or by temperature. These scenarios require further investigation.

Table S1 Crystal data collection and refinement details for $NbFeTe_2$

Parameter	Single-crystal	Polycrystalline
Refined composition	$NbFeTe_2$	
Formula weight	404	
Space group	$P2_1/c$ (No. 14)	
Diffractometer	Bruker D8 Quest	Huber G670
Detector	PHOTON III	Image plate
Radiation, λ (Å)	Mo$K\alpha$, 0.71073	Cu$K\alpha_1$, 1.5406
Refined parameters	57	42
2θ range (°)	2.79-33.4	3-100.3
Temperature (K)	293	
a (Å)	7.280(4)	7.2984(1)
b (Å)	6.305(4)	6.31110(7)
c (Å)	7.992(5)	7.99716(9)
β (°)	92.33(1)	92.279(1)
V (Å^3)	366.5(4)	368.067(9)
Z	4	
$\rho_{calc.}$ (g cm^{-3})	7.3206	7.2898
μ (cm^{-1})	22.416	180.589
Ranges in hkl	$-11 \le h \le 10$	$-7 \le h \le 7$
	$0 \le k \le 9$	$0 \le k \le 6$
	$0 \le l \le 11$	$0 \le l \le 7$
R_{int}	0.079	
R_1 [$I > 3\sigma(I)$]	0.0387	
wR_2 [$I > 3\sigma(I)$]	0.0475	
R1 (all)	0.0387	
wR$_2$ (all)	0.0475	
R_p		0.0314
R_{wp}		0.0422
R_{obs}		0.0427
wR_{obs}		0.0592
R_{all}		0.0427
wR_{all}		0.0592
GOF	1.21	2.32
Residual peaks (e$^-$ Å^{-3})	2.12/-2.07	1.58/-1.74

Table S2 Atomic position parameters in the crystal structure of $NbFeTe_2$

Atom*	x	y	z	U_{eq} (Å^2)
Single crystal				
Fe1	0.1108(2)	0.3534(2)	0.4955(2)	0.0157(5)
Nb1	0.0187(3)	0.5217(3)	0.1963(2)	0.0138(3)
Te1	0.3180(1)	0.2428(1)	0.25264(8)	0.0144(2)
Te2	0.2309(3)	0.7516(2)	-0.0292(2)	0.0159(2)
Polycrystalline				
Fe1	0.1130(4)	0.3637(3)	0.4858(3)	0.0159(9)
Nb1	0.0181(3)	0.5192(3)	0.1989(2)	0.0172(6)
Te1	0.3162(2)	0.2455(3)	0.2533(1)	0.0122(4)
Te2	0.2338(2)	0.7493(3)	-0.0296(1)	0.0134(5)

* All atoms fully occupy the 4*e* crystallographic sites

Table S3 Selected interatomic distances in the crystal structure of $NbFeTe_2$ according to the single crystal data

Atom1	Atom2	Distance (Å)
Fe1	-Fe1 (x1)	2.456(3)
	-Nb1 (x1)	2.676(4)
	-Nb1 (x1)	2.738(3)
	-Nb1 (x1)	2.786(4)
	-Nb1 (x1)	2.951(4)
	-Te1 (x1)	2.572(3)
	-Te1 (x1)	2.602(3)
	-Te2 (x1)	2.593(4)
	-Te2 (x1)	2.649(4)
Nb1	-Te1 (x1)	2.822(3)
	-Te1 (x1)	2.863(3)
	-Te2 (x1)	2.803(3)
	-Te2 (x1)	2.822(3)
	-Te2 (x1)	2.994(3)
	-Te2 (x1)	3.698(3)

Table S4 ^{57}Fe hyperfine parameters of $NbFeTe_2$,

T (K)	Component	δ (mm/s)	$\lvert eQV_{zz}\rvert$ (mm/s)	B_{hf} (T)	ϑ (°)	Γ (mm/s)	I (%)
300	Fe(1)	0.31(1)	1.15(1)	-	-	0.30(1)	94(2)
	Fe(2)	0.29(1)	1.63(6)	-	-	0.30(1)	6(2)
5	Fe(1)	0.43(1)	1.42(3)	9.77(4)	69.2(2)	0.33(1)	77(2)
	Fe(1A)	0.43(1)	1.42(3)	8.3(2)	64(1)	0.33(1)	15(2)
	Fe(2)	0.43(1)	1.68(11)	6.1(2)	59(2)	0.33(1)	8(2)

where δ is the isomer shift, eQV_{zz} – quadrupole interaction constant, B_{hf} – hyperfine magnetic field, ϑ – polar angle between the main component of the electric field gradient tensor and B_{hf}, Γ – full width at half maximum, and I – partial contribution.

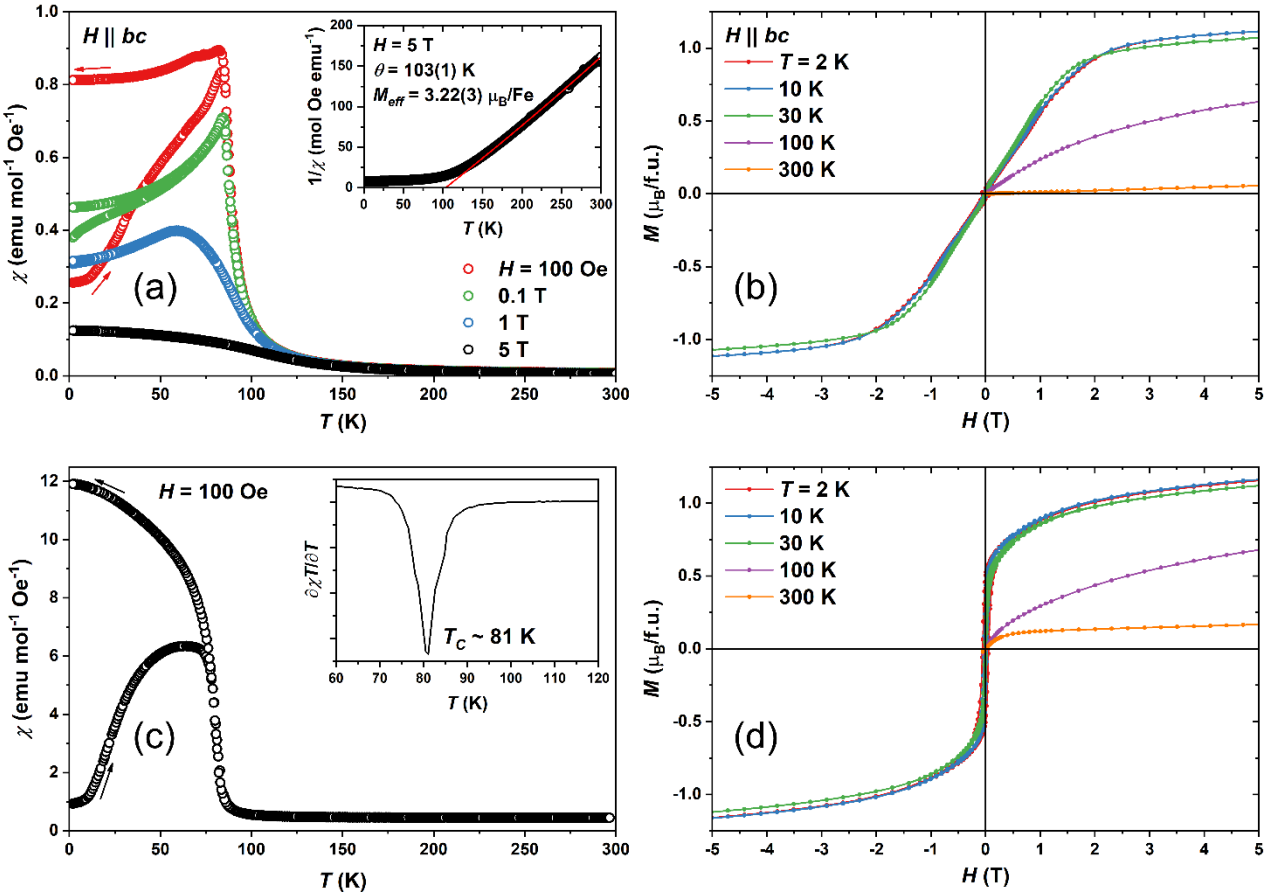

Figure S2 Magnetic properties of the $NbFeTe_2$ single crystal for H || bc (a) and (b), and polycrystalline sample (c) and (d). Magnetic susceptibility is shown in panels (a) and (c), and magnetization – in panels (b) and (d). The inset in (a) shows inverse susceptibility in 5 T magnetic field. The solid red line is a fit according to the modified Curie-Weiss law. The inset in (c) demonstrates the Fisher's heat capacity plot in 100 Oe magnetic field.

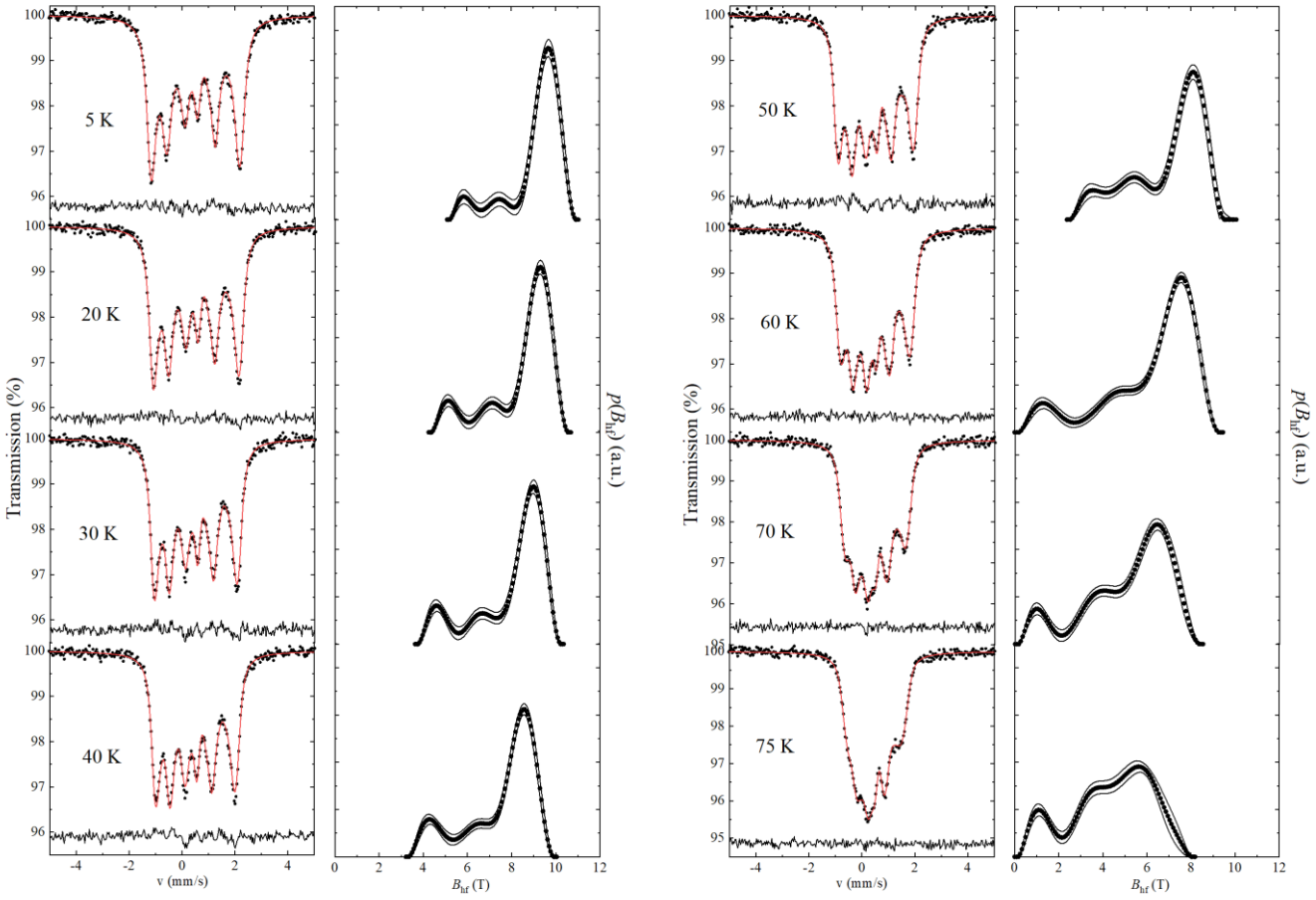

Figure S3 ^{57}Fe Mössbauer spectra of $NbFeTe_2$ in the magnetically ordered state fitted using a $p(B_{hf})$ distribution of the hyperfine magnetic fields (B_{hf}). The $p(B_{hf})$ distributions are shown on the right.

[1] V. Petříček, M. Dušek and L. Palatinus, *Z. Kristallogr.*, 2014, **229**, 345.
[2] K. Koepernik and H. Eschrig, *Phys. Rev. B*, 1999, **59**, 1743.
[3] J. P. Perdew, K. Burke and M. Ernzerhof, *Phys. Rev. Lett.*, 1996, **77**, 3865.
[4] P. E. Blöchl, O. Jepsen and O. K. Andersen, *Phys. Rev. B*, 1994, **49**, 16223.
[5] S. S. Starchikov, K. O. Funtov, V. A. Zayakhanov, K. V. Frolov, M. G. Klenov, I. Y. Bondarenko and I. S. Lyubutin, *Instrum. Exp. Tech.*, 2023, **66**, 497–507.
[6] M. E. Matsnev and V. S. Rusakov, *AIP Conf. Proc.*, 2012, **1489**, 178-185.
[7] A. V. Sobolev, A. A. Akulenko, I. S. Glazkova, A. A. Belik, T. Furubayashi, L. V. Shvanskaya, O. V. Dimitrova and I. A. Presniakov, *J. Phys. Chem. C*, 2018, **122**, 19767–19776.
[8] J. Li, M. E. Badding and F. J. DiSalvo, *Inorg. Chem.*, 1992, **31**, 1050–1054.
[9] J. Neuhausen, K.-L. Stork, E. Potthoff and W. Tremel, *Z. Naturforsch. B*, 1992, **47**, 1203–1212.